ACS Macro Letters

Letter

pubs.acs.org/macroletters

Confined Self-Assembly of Asymmetric Diblock Copolymers within Silica Nanobowl Arrays

Jie Yu, Chong Geng, Yiming Zeng, Qingfeng Yan,* Xiaoqing Wang, and Dezhong Shen

Department of Chemistry, State Key Laboratory of New Ceramics and Fine Processing, Tsinghua University, Beijing 100084, People's Republic of China

Supporting Information

ABSTRACT: The confined self-assembly of asymmetric diblock copolymer polystyrene-*block*-poly(methyl methacrylate) (PS-*b*-PMMA) within an array of silica nanobowls prepared using a colloidal spheres templating technique is investigated. By manipulation of the nanobowl size, block copolymer (BCP) thickness, and interfacial interaction, a rich variety of ordered BCP nanostructures not accessible in the bulk system or under other confinements are obtained, resulting in hierarchically ordered nanostructures.

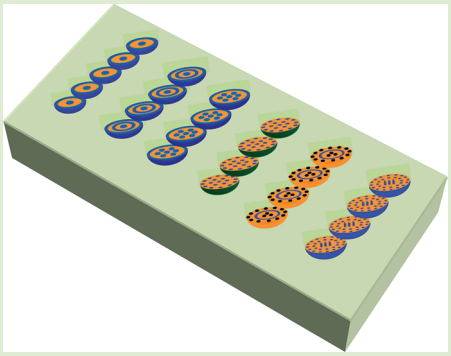

Diblock copolymer molecules consist of two chemically distinct blocks which are covalently linked to each other. Owing to their mutual repulsion, the two dissimilar blocks tend to segregate into different domains, and the spatial extent of the domains is limited by the constraint imposed by the covalent connectivity of the blocks, leading to a so-called microphase separation phenomenon.[1−8] The confinement provides a new route to develop unique self-assembled block copolymer (BCP) nanostructures which are not readily available in bulk or thin-film systems.[9−26] Compared to that in BCPs self-assembling under one-dimensional (1-D) and two-dimensional (2-D) confinements, polymer chains suffer more severe frustrations during microphase separation under three-dimensional (3-D) confinements. Thus, BCP self-assembly under 3-D confinements may experience unusual microphase separations which could lead to far more complex BCP nanostructures, as suggested by a number of theoretical predictions.[27−32]

Experimentally, Thomas and co-workers[33] first reported the self-assembly of lamella-forming diblock copolymer within a microdroplet. Okubo and co-workers[34−36] studied the microphase separation behaviors of BCP spheres. A diblock copolymer solution was emulsified to generate oil-in-water emulsions. As the volatile organic solvent evaporated, the BCP self-assembled into nanostructured spheres due to confined microphase separation. Yang and co-workers[37,38] also used an emulsion droplet as a confining geometry for the self-assembly of BCP−homopolymer blends. They have systematically investigated the effects of the particle size and the content of homopolymer on the internal morphology of the nanostructured spheres. Yabu and co-workers[39−46] have demonstrated a well-developed method, that is, self-organized precipitation, to produce micro/nanospheres from diblock copolymers or blends of diblock copolymers and homopolymers. During the formation of micro/nanospheres, self-assembly of diblock copolymer simultaneously occurs. Because of the 3-D spherical confinement, a diversity of microphase separation nanostructures both on the surface and within the inner core of the micro/nanospheres could be obtained. Besides direct synthesis of diblock copolymer spheres, colloidal templating strategy has been used to study the self-assembly of diblock copolymers under 3-D confinements. Using this strategy, Manners' group and Ozin's group have studied the confined self-assembly of symmetric polystyrene-*block*-poly(ferrocenylethylmethysilane) (PS-*b*-PFS) within silica spherical cavities and successfully generated concentric shell structures.[47] Subsequently, they systemically investigated the self-assembly of symmetric and asymmetric PS-*b*-PFS confined in silica colloidal crystals and inverse colloidal crystals.[48] Recently, Fu et al. fabricated ordered arrays of asymmetric pPolystyrene-*block*-poly(methyl methacrylate) (PS-*b*-PMMA) hollow spheres by using solution wetting of silica inverse colloidal crystals.[49] Microphase separation behaviors in these diblock copolymer hollow spheres were investigated. Nevertheless, all of the previous theoretical and experimental studies on 3-D confined self-assembly of diblock copolymers have focused on their microphase separation behaviors within a spherical cavity.

Here we report the microphase separation behaviors of asymmetric diblock copolymer PS-*b*-PMMA under 3-D confinement imposed by nanobowl arrays. The confining environment could be characterized into soft and hard confinement according to their deformability.[32] The size and shape of confining geometry are fixed in hard confinement such

Received: August 21, 2011
Accepted: October 5, 2011
Published: November 15, 2011

   dx.doi.org/10.1021/mz200032k | *ACS Macro Lett.* 2012, 1, 62−66

as an inverse colloidal crystal, whereas they are not fixed but deformable in soft confinement such as a microdroplet. Nanobowl arrays provide a unique 3-D confining system for the self-assembly of BCPs by combining the characteristic of soft and hard ones. The constraint imposed by the nanobowls is not as strong as that in the case of spherical hard confinement because it can be released by reorienting the polymer chains along the unconfined directions. It is also not as weak as that under soft confinement such as in a microdroplet because the shape of the underneath confining geometry is fixed. Furthermore, the interfacial interaction between the surface and the blocks are imposed not only at the inner wall of the nanobowls but also at the polymer/vacuum interface. These divergences induce BCPs to undergo different microphase separation behaviors in comparison with that under 3-D spherical hard confinement or microdroplet soft confinement, leading to new and complex copolymer morphologies which would not be accessible in the bulk system or under other confinements.

Figure 1 schematically illustrates the preparation of the silica nanobowl arrays and the confined self-assembly of diblock copolymer within the nanobowl arrays. Cylinder-forming asymmetric diblock copolymer PS-*b*-PMMA was selected in this study due to its promising potential for commercial applications.[50] In a typical process, a polystyrene colloidal monolayer was first fabricated from an air−water interface self-assembly approach.[51] The PS colloidal monolayer was transferred onto a silicon substrate and used as a template to construct a silica nanobowl array via the sol−gel method.[52] A brush of polystyrene-*random*-poly(methyl methacrylate) (PS-*r*-PMMA) or hydroxyl-terminated polystyrene (PS-OH) was anchored on the surface of the silica nanobowls. PS-*b*-PMMA dissolved in toluene was then spin-coated onto the substrate with a silica nanobowl array. BCP-coated samples were annealed at 170 °C for 48 h under vacuum and cooled subsequently to room temperature before taking out from the oven. To characterize the microphase separation nanostructures of the self-assembled diblock copolymer using a scanning electron microscope (SEM), the PMMA domain was selectively removed by exposuring to ultraviolet (UV) light irradiation and development with acetic acid.

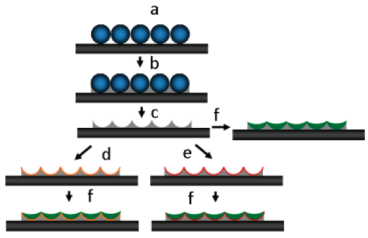

Figure 1. Schematic diagram of the confined self-assembly of diblock copolymer within a nanobowl array. (a) A PS colloidal monolayer was fabricated on a silicon substrate. (b) Silica sol was infiltrated into the interstices of the PS colloidal spheres. (c) PS colloidal spheres were removed, leaving behind an ordered silica nanbowl array. (d) The surface of the silica nanobowls was modified by a PS-OH brush. (e) The surface of the silica nanobowls was modified by a PS-*r*-PMMA brush. (f) BCP was spin-coated on the silica nanobowl array and self-assembled under thermal annealing.

The effect of the confining degree of silica nanobowls on the morphology of the self-assembled PS-*b*-PMMA diblock copolymer was investigated by altering the diameters of nanobowls. The confining degree d/L_0 is the ratio of confinement diameter d and equilibrium period L_0. The asymmetric PS-*b*-PMMA copolymer used in this study could form ordered hexagonally packed cylinder structure in the bulk system with a characteristic equilibrium period of around 32 nm.[53] The SEM images in Figure 2a−c are the microphase separation nanostructures of PS-*b*-PMMA confined in the silica nanobowls free of surface modification with various diameters from 98, 142, to 180 nm, with corresponding confinement degrees (d/L_0) of 3.0, 4.4, and 5.6. Figure 2d schematically illustrates the corresponding morphologies. It was observed that the resulting self-assembled BCP structures within the nanobowls were all center-symmetric. The reason lies in that with center-symmetrical confining geometries of nanobowls, the copolymer chains would be imposed to evenly disperse in the restricted confining space and gather into symmetrical structures to achieve the maximization of copolymer chain stretching.[28] In the case of silica nanobowls without surface modification, it was found that the PMMA blocks segregated to the polymer/silica interface due to the preferential affinity of PMMA to silica walls, forming the outermost layer of the center-symmetrical multilayer structure.[54,55] Figure 2a shows the morphology of the self-assembled PS-*b*-PMMA confined within 98 nm (d/L_0 = 3.0) silica nanobowls. It can be seen that a dot-like PMMA core was present at the center while the remaining space was filled with the PS domain. In the 142 nm (d/L_0 = 4.4) nanobowl confinement, a PMMA dot was formed at the center of each nanobowl as well. In addition, two extra center-symmetrical ring-like PMMA layers can be seen from the PS matrix (Figure 2b). By increasing the diameter of the nanobowls to180 nm (d/L_0 = 5.6), PMMA dots with a hexagonal symmetry formed in the PS matrix were obtained

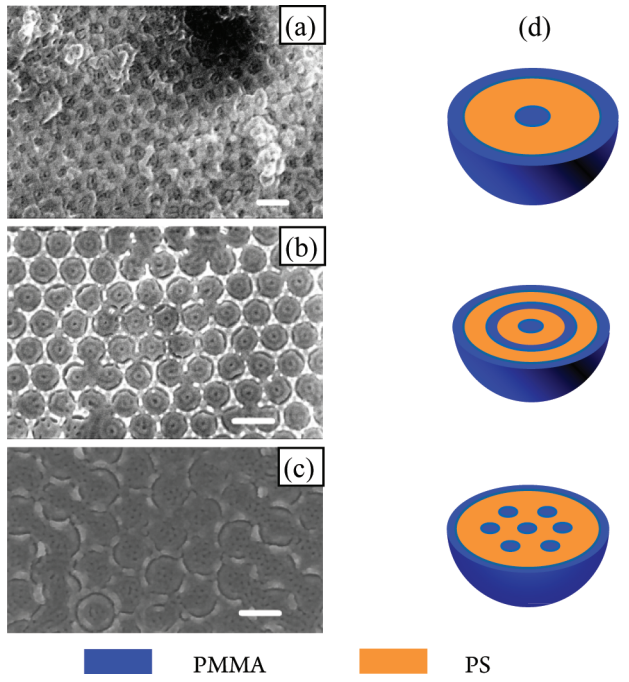

Figure 2. SEM images of morphologies of the self-assembled PS-*b*-PMMA confined in the silica nanobowl arrays with diameters of (a) 98 nm, (b) 142 nm, and (c) 180 nm. The yellow and blue regions denote the PS-rich and PMMA-rich phase, respectively. (d) Schematic illustrations of the BCP nanostructures within a silica nanobowl in a, b, and c, respectively. Scale bars are all 200 nm.

dx.doi.org/10.1021/mz200032k | *ACS Macro Lett.* 2012, 1, 62−66

(Figure 2c). According to previous theoretical and experimental studies,[25,28,48] it is believed that the PMMA dot could represent a solid sphere or a short cylinder, while the PMMA ring would exhibit a helical or toroid structure. The formation of these unconventional structures such as the dot and ring, which could not be produced from the bulk system, might be attributed to the forced curvature within the silica nanobowls and the confinement-induced entropy loss.[22,26] By comparing the morphologies of the self-assembled BCPs within silica nanobowls of three different diameters, it was found that, with increasing the nanobowl diameter, the resulting microphase separation nanostructures tended to become more complex. This is probably due to the reduced confining frustration and enhanced copolymer freedom in an increased confinement space. In addition, the self-assembled BCP nanostructures confined within 3-D nanobowls were different from those obtained under 3-D spherical confinement.[47−49] It might be caused by the constraint differences between entirely confined spheres and partially confined bowls, together with the interfacial interaction of both polymer/silica and polymer/vacuum presented in the nanobowl system. Therefore, it can be concluded that nanobowl arrays could be used as a new 3-D confinement to create unique microphase separation nanostructures which would enrich the repertoire of self-assembled BCP nanostructures.

In such a 3-D nanobowl array confining system, the thickness of the BCP film within the nanobowls would have significant influences on the final morphology. Figure 3 shows the SEM images of three typical BCP nanostructures formed at different regions along the silicon substrate surface with 562 nm nanobowls. The schematic illustrations of self-assembled BCP nanostructures confined in a single nanobowl are shown in the inserts in Figure 3. During the spin-coating process, various line spin speeds would be present along the surface, resulting in different thicknesses of BCPs within the silica nanobowls in various areas of the substrate. In the center area, the line spin speed was relatively slower than other regions, so that the thickness of the BCP filled at both the bottom and sidewall of each nanobowl would be relatively high. In the regions away from the center area of the substrate, the line spin speed was faster compared with that in the center region, leading to a reduced overall thickness of BCPs within each nanobowl. Less copolymer was distributed at the bottom compared with that at the sidewall. In the region further toward the edge of substrate, the spin speed would be even faster, which would further reduce the average BCP thickness. In this case, the base film would disappear, leaving behind a curved BCP thin film with a hole at the bottom. It is well-known that the PMMA blocks with a lower surface energy compared to PS blocks would preferentially wet the inner wall of the silica nanobowls, resulting in a parallel orientation of the microdomains. However, when the BCP film thickness was increased to a certain value, a transition from a parallel cylinder to a perpendicular cylinder phase would occur, as has been observed in the flat thin film system.[56] Therefore, for the thicker BCP within the nanobowls at the center region of the substrate, perpendicular PMMA cylinders were observed all over the nanobowls (Figure 3a). In Figure S1 in the Supporting Information (SI), a tilt top-view of the self-assembled BCP nanostructures was presented after the silica nanobowl template was removed by dilute hydrofluoric acid, which clearly indicates that the PMMA cylinders have penetrated the whole BCP film filled in the silica nanobowls. For the nanobowls away from the

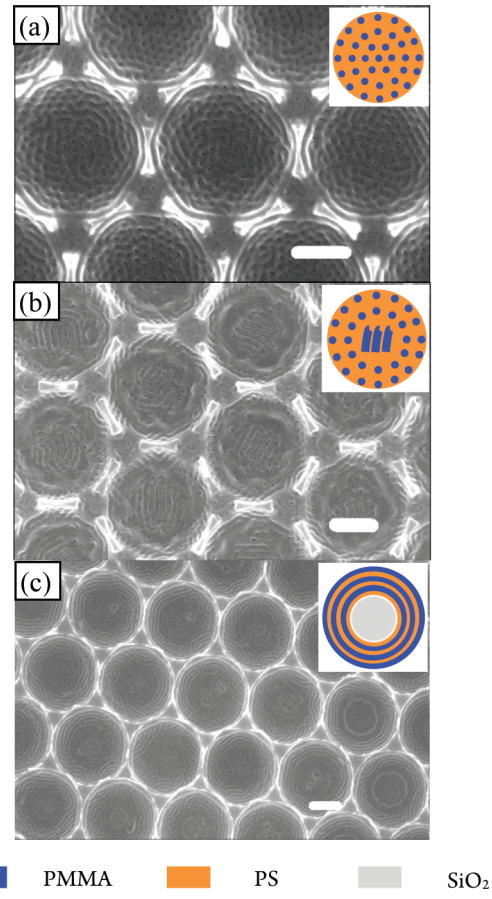

Figure 3. SEM images of the morphologies of the self-assembled PS-*b*-PMMA confined in the silica nanobowl arrays with a diameter of 562 nm located at different regions: (a) at the center of the substrate, (b) away from the center and toward the edge, and (c) at the edge of the substrate. The inserts are the schematic top views of the self-assembled BCP nanostructures. Scale bars are all 200 nm.

center, the film deposited at the sidewall was still thick enough to generate perpendicular PMMA cylinders, while the thinner portion at the bottom only provided parallel PMMA cylinders (Figure 3b). For the even thinner BCP within the nanobowls at the edge of the substrate, all of the cylinders would be oriented parallel to the surface of the sidewall, wrapping into concentric cylindrical domains under the nanobowl confinement (Figure 3c). Tilted side views of these self-assembled BCP nanostructures after the silica nanobowl templates were removed clearly and indicate the influence of the BCP film thickness on the morphology of the BCP nanostructures, as shown in Figure S2 in the SI. The transition of BCP nanostructures from perpendicular cylinders, a mixture of perpendicular and parallel cylinders, to concentric parallel cylinders was also observed in the silica nanobowls with a larger diameter. The SEM images shown in Figure S3 (see the SI) illustrate the similar transition of domain structure within 898 nm silica nanobowls when the thickness of BCP filled varied.

When confined within the silica nanobowls with different diameters, the BCP nanostructures exhibited different apparent periods. As shown in Figure S4 in the SI, when the diameters of the silica nanobowls were 180, 562, and 898 nm, the apparent period of the cylinders were approximately 40 nm, 37 nm, and 35 nm, respectively. All of these apparent periods were a little larger than the characteristic period obtained in bulk BCPs (L_0

dx.doi.org/10.1021/mz200032k | *ACS Macro Lett.* 2012, 1, 62−66

= 32 nm). Due to the variations in the nanobowl curvatures as well as the incommensurability between the confinement dimension and the characteristic cylinder period, the period of the self-assembled block domains would adjust to fulfill the boundary conditions, leading to different apparent periods within the silica nanobowls of different diameters. By increasing the nanobowl diameter, the curvature effects would be reduced, and the apparent period would be decreased to a value which was closer to the characteristic period in the bulk BCP deposited on a flat substrate. It could be predicted that, when the dimension of the silica nanobowls was further increased, the confinement effect would be reduced, and the microphase separation behavior of diblock copolymer under nanobowl confinement would perform similarly to that in a planar film system.

The effect of surface property of the nanobowls on the microphase separation nanostructures obtained was investigated by preanchoring the surface of 180 nm silica nanobowls with a PS-*r*-PMMA or PS-OH brush. Figure 4a shows the SEM image of the self-assembled BCP nanostructures within the silica nanobowls modified with a random brush, and Figure 4b is the corresponding schematic illustration. PMMA dots hexagonally packing in a PS matrix were observed, similar to the nanostructures formed within the silica nanobowls without surface modification (Figure 2c), except that the number of PMMA dots increased. In the case of the silica nanobowls without surface modification, because PMMA blocks had a lower surface interaction energy with silica, PMMA would prefer to migrate to the polymer/silica interface and form a ring-like PMMA layer there. As a result, the amount of PMMA block at the inner region decreased, leading to less PMMA dots formed. However, if the surface of silica nanobowl was modified by random brush to introduce a neutralized layer, such preferentially wetting of PMMA block would be prevented. More PMMA blocks would be present at the inner region, resulting in more PMMA dots emerging in the PS matrix. Figure 4c shows the SEM image of the self-assembled BCP nanostructures within the silica nanobowls modified with a PS brush, and Figure 4d is the corresponding schematic illustration. In this case, a three-layer structure was formed. In the inner layer, PMMA dots were distributed in the PS matrix symmetrically. In the middle layer, a ring-like PMMA layer appeared. In the outer layer, well-ordered PMMA dots symmetrically dispersed in the PS matrix were observed. These results implied that, if the surface of the nanobowls was neutral to both blocks, the microphase separation nanostructures became similar to those obtained in nanobowls with a surface attracting the minor component (PMMA block in our case). However, when the surface of the nanobowls attracted the major component (PS block in our case), the final structures would be different from those observed in a neutral surface system. These results were in agreement with the theoretical simulations on a spherical confinement system.[28]

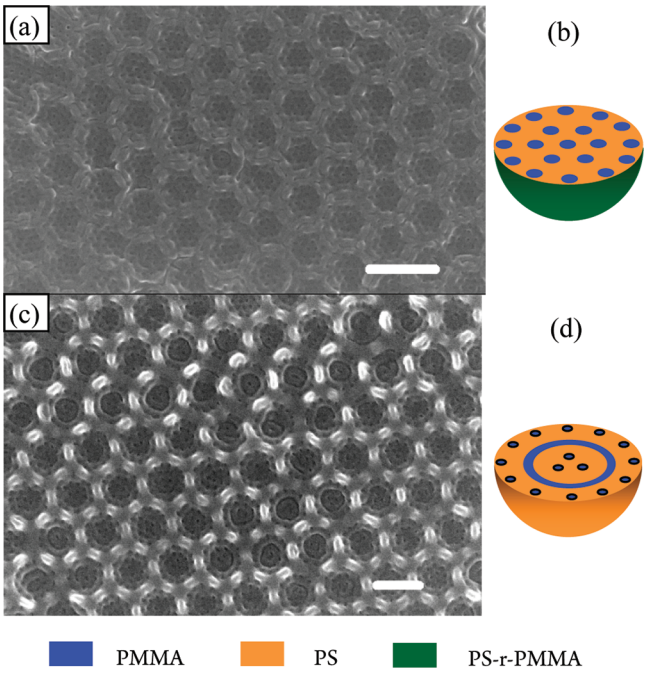

Figure 4. SEM images of the morphologies of the self-assembled PS-*b*-PMMA confined in 180 nm silica nanobowl arrays with surface modified by (a) PS-*r*-PMMA and (c) PS-OH. (b and d) Schematic illustrations of the BCP nanostructure in a single nanobowl corresponding to a and c, respectively. Scale bars in a and b are 300 nm and 200 nm, respectively.

In summary, nanobowl arrays provide a unique 3-D confining system for the self-assembly of cylinder-forming PS-*b*-PMMA. The nanobowl size, the BCP film thickness within the nanobowls, and the surface interactions strongly influenced the microphase separation nanostructures of the self-assembled diblock copolymer nanostructure. Under the nanobowl confinement, unusual morphologies such as ring and cylinder packing in a circle shape could be observed. When the thickness of the BCP within the nanobowls varied, various self-assembled BCP morphologies appeared. Furthermore, increasing the nanobowl diameter would reduce the curvature effect, resulting in a decrease of the apparent period of the BCP domains and a self-assembled morphology more similar to that obtained in a BCP film deposited on a flat substrate. In previous spherical confinements imposed either by an inversed colloidal crystal or a microdroplet, the confinement imposed is symmetric and isotropic. In this work, the confinement imposed by the nanobowl is anisotropic. The anisotropic confined shape might play an important role during the confined self-assembly of BCP. The manipulation of the surface interactions could lead to different self-assembled nanostructures. By controlling the nanobowl size, BCP thickness, and interfacial interaction, a rich variety of ordered nanostructures not accessible in bulk BCPs and under other confinements were obtained. Integration with the highly ordered nanobowl arrays leads to hierarchically ordered nanoscopic structures, which may find applications in optoelectronic devices, microfluidic devices, biomedical science, field emission, and so forth.[57−59]

■ ASSOCIATED CONTENT

Ⓢ Supporting Information

Experimental details and further information on microphase separation BCP nanostructures within silica nanobowls. This material is available free of charge via the Internet at http://pubs.acs.org.

■ AUTHOR INFORMATION

Corresponding Author

*E-mail: yanqf@mail.tsinghua.edu.cn.

Notes

The authors declare no competing financial interest.

dx.doi.org/10.1021/mz200032k | *ACS Macro Lett.* 2012, 1, 62−66

■ ACKNOWLEDGMENTS

This work was supported by the Natural Science Foundation of China (Project Nos. 50903046, 51173097), the Fok Ying Tung Education Foundation (Project No. 122018), and the Research Fund for the Doctoral Program of Higher Education of China (Project No. 20090002120043). The authors thank Professors X. Zhang and H. Xu from the Department of Chemistry, Tsinghua University, People's Republic of China, for their kind help on UV exposure experiments.

■ REFERENCES

(1) Bates, F. S.; Fredrickson, G. H. *Phys. Today* **1999**, *52*, 32.
(2) Mansky, P.; Harrison, C. K.; Chaikin, P. M.; Register, R. A.; Yao, N. *Appl. Phys. Lett.* **1996**, *68*, 2586.
(3) Urbas, A.; Sharp, R.; Fink, Y.; Thomas, E. L.; Xenidou, M.; Fetters, L. J. *Adv. Mater.* **2000**, *12*, 812.
(4) Thurn-Albrecht, T.; Steiner, R.; DeRouchey, J.; Stafford, C. M.; Huang, E.; Bal, M.; Tuominen, M.; Hawker, C. J.; Russell, T. P. *Adv. Mater.* **2000**, *12*, 787.
(5) Yang, S. Y.; Ryu, I.; Kim, H. Y.; Kim, J. K.; Jang, S. K.; Russell, T. P. *Adv. Mater.* **2006**, *18*, 709.
(6) Yoon, J.; Lee, W.; Thomas, E. L. *Nano Lett.* **2006**, *6*, 2211.
(7) Li, Q.; Lau, K. H. A.; Sinner, E.-K.; Kim, D. H.; Knoll, W. *Langmuir* **2009**, *25*, 12144.
(8) Bang, J.; Jeong, U.; Ryu, D. Y.; Russell, T. P.; Hawker, C. J. *Adv. Mater.* **2009**, *21*, 4769.
(9) Stewart-Sloan, C. R.; Thomas, E. L. *Eur. Polym. J.* **2011**, *47*, 630.
(10) Huinink, H. P.; Brokken-Zijp, J. C. M.; van Dijk, M. A.; Sevink, G. J. A. *J. Chem. Phys.* **2000**, *112*, 2452.
(11) Wang, Q.; Nealey, P. F.; de Pablo, J. J. *Macromolecules* **2001**, *34*, 3458.
(12) Xu, T.; Hawker, C. J.; Russell, T. P. *Macromolecules* **2005**, *38*, 2802.
(13) Ludwigs, S.; Krausch, G.; Magerle, R.; Zvelindovsky, A. V.; Sevink, G. J. A. *Macromolecules* **2005**, *38*, 1859.
(14) Park, I.; Park, S.; Park, H. W.; Chang, T.; Yang, H. C.; Ryu, C. Y. *Macromolecules* **2006**, *39*, 315.
(15) Chen, P.; Liang, H. *J. Phys. Chem. B* **2006**, *110*, 18212.
(16) Xiang, H.; Shin, K.; Kim, T.; Moon, S. I.; McCarthy, T. J.; Russell, T. P. *Macromolecules* **2004**, *37*, 5660.
(17) Shin, K.; Xiang, H. Q.; Moon, S. I.; Kim, T.; McCarthy, T. J.; Russell, T. P. *Science* **2004**, *306*, 76.
(18) Xiang, H.; Shin, K.; Kim, T.; Moon, S.; McCarthy, T. J.; Russell, T. P. *J. Polym. Sci., Part B: Polym. Phys.* **2005**, *43*, 3377.
(19) Yamaguchi, T.; Yamaguchi, H. *Adv. Mater.* **2008**, *20*, 1684.
(20) Sevink, G. J. A.; Zvelindovsky, A. V.; Fraaije, J. G. E. M.; Huinink, H. P. *J. Chem. Phys.* **2001**, *115*, 8226.
(21) Wu, Y.; Cheng, G.; Katsov, K.; Sides, S. W.; Wang, J.; Tang, J.; Fredrickson, G. H.; Moskovits, M.; Stucky, G. D. *Nat. Mater.* **2004**, *3*, 816.
(22) Yu, B.; Sun, P.; Chen, T.; Jin, Q.; Ding, D.; Li, B. *Phys. Rev. Lett.* **2006**, *96*, 138306.
(23) Chen, P.; He, X.; Liang, H. *J. Chem. Phys.* **2006**, *124*, 104906.
(24) Feng, J.; Ruckenstein, E. *Macromolecules* **2006**, *39*, 4899.
(25) Yu, B.; Sun, P.; Chen, T.; Jin, Q.; Ding, D.; Li, B.; Shi, A.-C. *Chem. Phys.* **2007**, *126*, 024903.
(26) Yu, B.; Jin, Q.; Ding, D.; Li, B.; Shi, A.-C. *Macromolecules* **2008**, *41*, 4042.
(27) Yu, B.; Li, B.; Jin, Q.; Ding, D.; Shi, A.-C. *Macromolecules* **2007**, *40*, 9133.
(28) Chen, P.; Liang, H.; Shi, A.-C. *Macromolecules* **2008**, *41*, 8938.
(29) Huh, J.; Park, C.; Kwon, Y. K. *J. Chem. Phys.* **2010**, *133*, 114903.
(30) Li, S.; Liu, M.; Ji, Y.; Zhang, L.; Liang, H. *Polym. J.* **2011**, *43*, 606.
(31) Li, S.; Chen, P.; Zhang, L.; Liang, H. *Langmuir* **2011**, *27*, 5081.
(32) Chi, P.; Wang, Z.; Li, B.; Shi, A.-C. *Langmuir* **2011**, *27*, 11683.
(33) Thomas, E. L.; Reffner, J. R.; Bellare, J. *J. Phys. Colloq.* **1990**, *51*, C7363.
(34) Okubo, M.; Saito, N.; Takekoh, R.; Kobayashi, H. *Polymer* **2005**, *46*, 1151.
(35) Tanaka, T.; Saito, N.; Okubo, M. *Macromolecules* **2009**, *42*, 7423.
(36) Kitayama, Y.; Kagawa, Y.; Minami, H.; Okubo, M. *Langmuir* **2010**, *26*, 7029.
(37) Jeon, S.-J.; Yi, G.-R.; Koo, C. M.; Yang, S.-M. *Macromolecules* **2007**, *40*, 8430.
(38) Jeon, S.-J.; Yi, G.-R.; Yang, S.-M. *Adv. Mater.* **2008**, *20*, 4103.
(39) Yabu, H.; Higuchi, T.; Shimomura, M. *Adv. Mater.* **2005**, *17*, 2062.
(40) Higuchi, T.; Yabu, H.; Onoue, S.; Kunitake, T.; Shimomura, M. *Colloids Surf., A* **2008**, *313*−*314*, 87.
(41) Higuchi, T.; Tajima, A.; Yabu, H.; Shimomura, M. *Soft Matter* **2008**, *4*, 1302.
(42) Higuchi, T.; Tajima, A.; Motoyoshi, K.; Yabu, H.; Shimomura, M. *Angew. Chem., Int. Ed.* **2008**, *47*, 8044.
(43) Higuchi, T.; Tajima, A.; Motoyoshi, K.; Yabu, H.; Shimomura, M. *Angew. Chem., Int. Ed.* **2009**, *48*, 5125.
(44) Li, L.; Matsunaga, K.; Zhu, J.; Higuchi, T.; Yabu, H.; Shimomura, M.; Jinnai, H.; Hayward, R. C.; Russell, T. P. *Macromolecules* **2010**, *43*, 7807.
(45) Higuchi, T.; Motoyoshi, K.; Sugimori, H.; Jinnai, H.; Yabu, H.; Shimomura, M. *Macromol. Rapid Commun.* **2010**, *31*, 1773.
(46) Yabu, H.; Motoyoshi, K.; Higuchi, T.; Shimomura, M. *Phys. Chem. Chem. Phys.* **2010**, *12*, 11944.
(47) Arsenault, A. C.; Rider, D. A.; Tetreault, N.; Chen, J. I. L.; Coombs, N.; Ozin, G. A.; Manners, I. *J. Am. Chem. Soc.* **2005**, *127*, 9954.
(48) Rider, D. A.; Chen, J. I. L.; Eloi, J.-C.; Arsenault, A. C.; Russell, T. P.; Ozin, G. A.; Manners, I. *Macromolecules* **2008**, *41*, 2250.
(49) Fu, J.; Wang, J.; Li, Q.; Kim, D. H.; Knoll, W. *Langmuir* **2010**, *26*, 12336.
(50) Joona, B.; Unyong, J.; Du, Y. R.; Thomas, P. R.; Craig, J. H. *Adv. Mater.* **2009**, *21*, 4769.
(51) Yu, J.; Yan, Q.; Shen, D. *ACS Appl. Mater. Interfaces* **2010**, *2*, 1922.
(52) Zhou, Z.; Zhao, X. S. *Langmuir* **2005**, *21*, 4717.
(53) Tada, Y.; Akasaka, S.; Yoshida, H.; Hasegawa, H.; Dobisz, E.; Kercher, D.; Takenaka, M. *Macromolecules* **2008**, *41*, 9267.
(54) Russell, T. P.; Menelle, A.; Anastasiadis, S. H.; Satija, S. K.; Majkrzak, C. F. *Macromolecules* **1991**, *24*, 6263.
(55) Kim, H.-C.; Russell, T. P. *J. Polym. Sci., Part B: Polym. Phys.* **2001**, *39*, 663.
(56) Zhang, X.; Berry, B. C.; Yager, K. G.; Kim, S.; Jones, R. L.; Satija, S.; Pickel, D. L.; Douglas, J. F.; Karim, A. *ACS Nano* **2008**, *2*, 2331.
(57) Morariu, M.; Voicu, N.; Schäffer, E.; Lin, Z.; Russell, T. P.; Steiner, U. *Nat. Mater.* **2003**, *2*, 48.
(58) Meng, G. W.; Jung, Y. J.; Cao, A. Y.; Vajtai, R.; Ajayan, P. M. *Proc. Natl. Acad. Sci. U.S.A.* **2005**, *102*, 7074.
(59) Li, Y.; Li, C.; Cho, S. O.; Duan, G.; Cai, W. *Langmuir* **2007**, *23*, 9802.